

BJR

■ **BIOMECHANICS**

# Marker free model-based radio-stereometric analysis for evaluation of hip joint kinematics

A VALIDATION STUDY

**L. Hansen,  
S. De Raedt,  
P. B. Jørgensen,  
B. Mygind-Klavsen,  
B. Kaptein,  
M. Stilling**

*Orthopaedic Research Unit, Department of Orthopaedics, Aarhus, Denmark*

■ L. Hansen, MD, First-year Resident, Department of Internal Medicine, Central Hospital of Holstebro, Holstebro, Denmark and Orthopaedic Research Unit, Aarhus University Hospital, Aarhus C, Denmark.

■ S. De Raedt, MSc, PhD, Development Engineer, Nordisk Røntgen Teknik, Hasselager, Denmark and Orthopaedic Research Unit, Aarhus University Hospital, Aarhus C, Denmark.

■ P. B. Jørgensen, MSc, PhD Student, Orthopaedic Research Unit, Aarhus University Hospital Aarhus C, Denmark and Department of Clinical Medicine, Aarhus University, Aarhus N, Denmark.

■ B. Mygind-Klavsen, MD, Sports Surgeon, Department of Orthopaedic Surgery, Aarhus University Hospital, Aarhus C, Denmark.

■ B. Kaptein, MSc, PhD, Senior Researcher, Biomechanics and Imaging Group, Department of Orthopaedic Surgery, Leiden University Medical Center, Leiden, The Netherlands.

■ M. Stilling, MD, PhD, Associate Professor, Department of Orthopaedic Surgery, Aarhus University Hospital, Aarhus C, Denmark and Department of Clinical Medicine, Aarhus University, Aarhus N, Denmark.

Correspondence should be sent to L. Hansen; email: larshansen33@hotmail.com

doi: 10.1302/2046-3758.76.BJR-2017-0268.R1

*Bone Joint Res* 2018;7:379–387.

## Objectives

To validate the precision of digitally reconstructed radiograph (DRR) radiostereometric analysis (RSA) and the model-based method (MBM) RSA with respect to benchmark marker-based (MM) RSA for evaluation of kinematics in the native hip joint.

## Methods

Seven human cadaveric hemipelvises were CT scanned and bone models were segmented. Tantalum beads were placed in the pelvis and proximal femoral bone. RSA recordings of the hips were performed during flexion, adduction and internal rotation. Stereoradiographic recordings were all analyzed with DRR, MBM and MM. Migration results for the MBM and DRR with respect to MM were compared. Precision was assessed as systematic bias (mean difference) and random variation (Pitman's test for equal variance).

## Results

A total of 288 dynamic RSA images were analyzed. Systematic bias for DRR and MBM with respect to MM in translations ( $p < 0.018$  mm) and rotations ( $p < 0.009^\circ$ ) were approximately 0. Pitman's test showed lower random variation in all degrees of freedom for DRR compared with MBM ( $p < 0.001$ ).

## Conclusion

Systematic error was approximately 0 for both DRR or MBM. However, precision of DRR was statistically significantly better than MBM. Since DRR does not require marker insertion it can be used for investigation of preoperative hip kinematics in comparison with the postoperative results after joint preserving hip surgery.

**Cite this article:** *Bone Joint Res* 2018;7:379–387.

**Keywords:** Radiostereometric analysis, Hip, Kinematics

## Article focus

■ To validate the precision of digitally reconstructed radiograph (DRR) radiostereometric analysis (RSA) and model-based RSA with respect to benchmark marker-based RSA for the native hip joint.

## Key messages

- DRR-based RSA is a highly precise method for investigating hip joint kinematics both preoperatively and after hip joint preserving surgery.
- DRR-based RSA is a non-invasive method for investigating hip joint kinematics.
- DRR-based RSA can be applied to other joints with equally high precision.

## Strengths and limitations

- Strong validation, multiple stereoradiographic analysis, using seven donor hips in clinically relevant positions.
- Analysis of DRRs is computer automated and not influenced by the analyst.
- High radiation dose when using bone models might limit the study's applicability.

## Introduction

Exact evaluation of hip joint kinematics is valuable for understanding the pathomechanics of joint instability and mechanical obstructions such as those related to hip dysplasia or Cam- and pincer femoroacetabular impingement (FAI). A non-invasive method to evaluate the pre- and postoperative kinematics of



Fig. 1

Image showing the segmented models of the pelvic and the femur bone.

these hip conditions is warranted. Radiostereometric analysis (RSA) is an accurate method for tracking 3D movements of objects and may be used to track moving bones and joint kinematics. Marker-based RSA or the 'marker method' (MM) uses tantalum marker beads inserted into the bone. Movements of the markers can be followed very accurately during RSA recordings, and MM is widely used for monitoring implant fixation and wear to sub-millimetre precision.<sup>1-3</sup> However the need for marker insertion limits the clinical application of MM to postoperative evaluations. Therefore, there is a real need for developing marker-less methods for analysis of stereoradiographs. Analysis by a model-based method (MBM) with software (model-based RSA (MBRSA); *RSAcore*, Leiden, Netherlands) is semi-automated and is performed by matching of triangulated surface bone models, obtained from CT data, to manually selected contours. MBM has typically been used to analyze implant fixation by use of implant computer-aided design models.<sup>4,5</sup> However, CT-constructed bone models may also be used for MBM, which makes it possible to evaluate *in vivo* joint kinematics without markers.<sup>6-8</sup> Analysis with MBRSA though is time consuming as it requires manual user interaction. A second method for analysis of stereoradiographs is by use of digitally reconstructed radiographs (DRR).<sup>9</sup> The DRR RSA method works by comparing the simulated DRR images with the RSA radiographs. The analyses are then performed using automated software developed at our institution (*AutoRSA* software; Orthopaedic Research Unit, Aarhus, Denmark), which allows for automated analyses and eliminates the need for interactive analysis.

Many other factors such as exposure, image resolution, contrast, model accuracy, overlapping bones/contours, patient position and equipment setup can

influence the precision of an RSA analysis. Furthermore, the amount of soft tissue that the radiographs needs to penetrate may influence image quality and thereby affect precision. It is therefore important to conduct a validation study to assess method precision for a specific anatomical region prior to initiating clinical studies.

The aim of this study was to validate the precision of two non-invasive analysis methods, MBM and DRR, against the benchmark MM for precise tracking of *in vivo* bone movements of the hip joint in dynamic radiostereometric images. We hypothesized that MBM and DRR are precise methods for tracking hip joint bone movements and that that DRR would have superior precision.

## Materials and Methods

Seven human cadaveric legs with hemipelves were acquired for the study (Department of Biomedicine, Aarhus University). The donors ranged from 58 to 94 years of age, four were female and three were male. The study was approved by The Central Denmark Region Committees on Health Research Ethics (case number 1-10-72-6-16 issued on 24 February 2016). No power calculation was performed because no other studies in the literature were available for comparison. The number of specimens included was chosen based on experience from a previous validation study on the knee performed using the same system.<sup>10</sup>

Donor legs were scanned in a clinical CT scanner (Brilliance 64; Philips Healthcare, Cleveland, Ohio). Settings were 120 kV, 150 mAs, slice thickness 2.5 mm and slice increment 1.25 mm using a helical scan protocol with reconstruction kernel 'C'. Bones were segmented from the CT scans using a custom implemented fully automated graph-cut segmentation method<sup>11,12</sup> employing the Insight Segmentation and Registration Toolkit (Kitware, Clifton Park, New York). This method uses eigen analysis of the hessian matrix to identify the sheet-like structure of the bone surface. Subsequently, a sheetness measure is formulated, which is used in a graph-cut optimization.<sup>13</sup>

Segmentations of the pelvis included the iliac, ischial and pubic bone. All segmentations were visually inspected and verified to be within voxel accuracy (< 0.3 mm). The femur models included the femoral head, neck and proximal 7 cm distal to the lesser trochanter (Fig. 1). From the segmentations, both volume and surface bone models were created for use with the DRR and MBM analysis, respectively. The volume model consisted of the extracted bone containing the grey scale information of the CT scan. The surface model was extracted using the marching cubes algorithm and simplified to 10 000 triangular elements using Visualization Toolkit (Kitware).

Local coordinate systems were created for all bone models. The femoral coordinate system is defined according to the International Society of Biomechanics recommendations:<sup>14</sup> from the centre of the femoral head, with

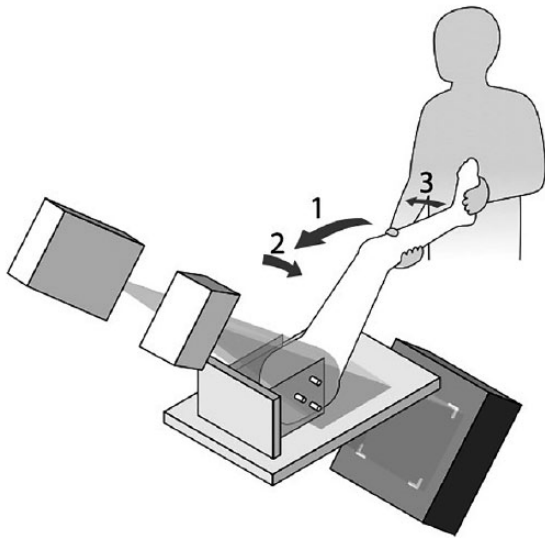


Fig. 2

Setup of the radiostereometric equipment. The radiograph tubes are positioned with a 20° mediolateral and 45° cranio-caudal tilt. The calibration box is placed in a 45° angle beneath the hip joint. The arrows indicate the movement 1) flexion, 2) adduction and 3) internal rotation. Reprinted with courtesy from Hansen et al.<sup>6</sup>

the y-axis defined as a line through the femoral epicondyle, the z-axis as the line perpendicular to the y-axis, in the plane defined by the two femoral epicondyles, and orientated to the right. Lastly the x-axis is defined as the line perpendicular to the y- and z-axis orientated anteriorly. Equally, the pelvic coordinate system is defined from the centre of the femoral head with the z-axis defined as a line parallel to the line between the two anterior superior iliac spines (ASIS), orientated to the right. The x-axis is defined as a line orthogonal to the z-axis and parallel to a line in the plane defined by the two ASISs and the midpoint of the two posterior superior iliac spines. Finally, the y-axis is defined as a line pointing cranially and perpendicular to the x- and z-axis.<sup>15</sup>

**Experimental setup and equipment.** Prior to RSA recordings, 0.8-mm tantalum marker beads were inserted into the bones using a bead gun (Kulkanon, Wennbergs Finmek, Sweden). Eight to ten markers were placed in the proximal femur through a hole in the lesser trochanter and were distributed from the greater trochanter to 2 cm distal to the lesser trochanter. Eight to ten markers were placed in the pelvis anterior and superior to the acetabulum through a hole drilled in the pectineal line. To ensure high quality MM-analyses, markers were distributed in approximately the same pattern in all donor legs and in a manner creating the largest possible matrix.

Fixtures for the hemipelvis were constructed for RSA recordings (Fig. 2). The hemipelvis were mounted in a portable fixture consisting of two 8-mm acrylic plates (manufacturer unknown) attached to a plywood board. The width between the acrylic glass plates could be

adjusted and the hemipelvis were mounted and fixed by use of three spiral drills through the ilium and the sacrum.

Dynamic stereoradiographs were recorded using a fully digital RSA system (Adora RSAd; NRT-Xray, Farsø, Denmark). Images were acquired at 5 frames/sec for dynamic recordings. The portable hemipelvis fixture was fixed to the radiography table (Fig. 2). The roentgen tubes were positioned with a 20° mediolateral and 45° cranio-caudal tilt, shooting at the hip joint from the cranial end and pointing caudally. Beneath the radiography table a uniplanar calibration box (Carbonbox 14; Medis Specials, Leiden, Netherlands) was placed at a 45° angle to the horizontal plane. The two image detectors (Canon CXDI-50RF; Canon, Amstelveen, The Netherlands) were slotted in behind the calibration box. Source image distance was 2220 mm and focus skin distance 1140 mm. Exposure settings for recordings were 130 kV, 500 mA, 16 mAS and resolution was  $2208 \times 2688$  pixels (79 DPI).

**Test protocol.** The donor legs were set to thaw at 5°C 120 hours before testing. Prior to the first recording the donor legs were mounted in the portable fixture and to the radiology table for the initial RSA recordings. One dynamic stereoradiographic recording (approximately 5 seconds and 25 images per movement) of a full flexion, adduction and internal rotation (FADIR) movement (i.e. a movement of the hip from full extension to flexion, adduction and internal rotation, then external rotation, abduction and extension) was recorded for each specimen (Fig. 2). The FADIR test is, according to The Warwick Agreement<sup>16</sup> on FAI syndrome, the most well-known test and is sensitive but not specific. When using the FADIR test it was possible to detect changes in internal rotation where FAI patients often have restricted range of movement. The donor leg was then moved off the recording table, remounted and dynamic RSA was repeated, tests 1 and 2, respectively.

**Analysis of radiographs.** The stereoradiographs were analyzed by MM, MBM and DRR methods. For calibration of the stereoradiographic images and for analysis the commercially available software (Model-Based RSA, v.4.02; RSAcore) was used.

**Calibration.** All stereoradiographic images were calibrated by identifying the fiducial and control markers of the calibration box in the images. The fiducial markers are used for determining the roentgen foci (the projections).<sup>3</sup> Based on the known marker grid in the calibration box, a laboratory coordinate system is defined (fiducial markers) and the positions of the roentgen foci are determined (control markers). The first image in a dynamic recording was calibrated and the same calibration was then used in subsequent images as no change in the set-up happens during the short dynamic RSA recording.<sup>10,27</sup> Analysis by all methods was performed on the same images and the calibration was identical for all methods, hence the

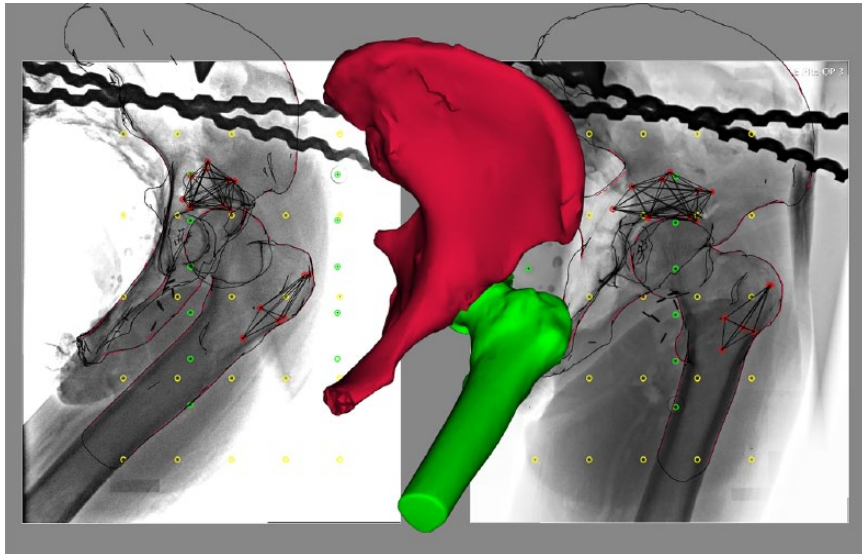


Fig. 3

Bone models fitted by projection to the radiographical contours in model-based radiostereometric software (RSAcore, Leiden, Netherlands). Control and fiducial markers in the calibration box are identified and labelled with green and yellow circles respectively.

observed migration differences between methods are not influenced by differences in calibration.

**MM RSA.** The inserted bone markers were identified in all corresponding images. Identification of markers is semi-automated in MBRSA, limiting the impact and number of observer-related errors. The position of identified markers in the coordinate system defined by the calibration box is calculated, allowing for the marker matrix to be tracked. As markers are rigid bone markers that appear as high contrast in the images, MM can be used as a highly accurate reference for comparison with bone positions determined with MBM and DRR.

**MM analysis quality.** High quality MM analyses relies on adequately inserted marker beads which can be estimated using the mean error of rigid body matching (ME) and condition number.<sup>2</sup> The stability of the inserted markers can be estimated by calculating the ME, which describes the mean difference in relative distances between the inserted markers, using the previous scenes (RSA images) as the reference. The recommended upper limit of ME is 0.35 mm.<sup>17</sup> The distribution of markers is commonly described using the condition number. The condition number is computed using the geometry of the marker matrix, with low condition numbers indicating proper distribution. To obtain very reliable results studies have shown that condition numbers should be below 100-110.<sup>17</sup> To track the 3D marker position of an object/bone accurately, a minimum of three beads are required for analysis<sup>19</sup> but accuracy increases with the number of detected markers and their distribution.<sup>17,18</sup>

**MBM RSA.** Contours were automatically detected in the stereoradiographs by the MBRSA software using the Canny Edge Detector (RSAcore, Leiden, The Netherlands). The bone contours of the pelvis and femur were then

manually selected from these detected contours. Identification of contours was made meticulously and standardized for all donor legs in all images. For the femur the identified contours included approximately 15 cm of the proximal diaphysis, the lesser and greater trochanter, the femoral neck and parts of the femoral head. Identified contours on the pelvis included the pubic and ischial rami, the ischial spine and the iliac crest. The CT-constructed bone models were imported into the MBRSA software, which automatically positioned the bone models according to the marked contours following three consecutive algorithms: IIPM, DIFDHSann and DIFDoNLP. These algorithms estimate the pose by minimizing error between the virtual projections of the bone models and the manually selected contours (Fig. 3).<sup>20</sup>

**DRRs.** The automated DRR analysis is based on intensity-based 2D/3D image registration using the volume model. In summary, the 3D bone volume from the CT scan is used to simulate images which are subsequently compared with the RSA images using a similarity metric. The position and orientation that minimizes the similarity metric corresponds to the optimum position. Based on initial tests and in accordance to the findings of van der Bom et al,<sup>21</sup> we found that the best metric was the normalized gradient correlation. Since movements between successive frames can be large, we employed a two-stage registration using a global optimizer at quarter resolution and subsequently a local optimizer at full resolution. The lower resolution significantly speeds up the initial global optimization which requires more iterations. The analysis was performed using a modified version of Elastix (Elastix, Madrid, Spain)<sup>22</sup> and support for the nonlinear optimization library NLOpt (Steven G. Johnson, Boston, Massachusetts) was integrated. For the initial registration



**Table I.** Model-based radiostereometric analysis (RSA); mean difference in translation errors, n = 288

	Femur				Pelvis			
	Tx	Ty	Tz	Total	Tx	Ty	Tz	Total
Mean difference*	0.005	0.014**	-0.002	0.213	-0.002	0.003	0.006	0.355
SD difference†	0.075	0.106	0.226	0.150	0.107	0.158	0.462	0.351
± LoA‡	0.146	0.208	0.443	0.293	0.209	0.310	0.905	0.688
Minimum§	-0.235	-0.312	-0.829	0.025	-0.381	-0.627	-1.499	0.002
Maximum¶	0.290	0.414	0.669	0.868	0.436	0.648	1.933	1.958

\*mean difference in translations (mm) between model-based method RSA and marker method RSA

†SD of the mean difference, random variation

‡limits of agreement (LoA) 95%, expected clinical precision

§minimum observed value

¶maximum observed value

\*\*statistically significantly different from 0, paired *t*-test

Tx, Ty and Tz: mean difference in translation errors along the x-, y- and z-axis, respectively

**Table II.** Model-based radiostereometric analysis (RSA); mean difference in rotation errors, n = 288

	Femur				Pelvis			
	Rx	Ry	Rz	Total	Rx	Ry	Rz	Total
Mean difference*	-0.001	-0.007	-0.01	0.400	0.008	-0.009	-0.009	0.334
SD difference†	0.267	0.361	0.188	0.276	0.296	0.201	0.243	0.275
± LoA‡	0.523	0.707	0.369	0.542	0.580	0.394	0.477	0.539
Minimum§	-0.738	-1.619	-0.620	0.016	-1.095	-0.629	-1.177	0.018
Maximum¶	1.048	1.285	0.669	1.689	1.398	0.679	0.962	1.539

\*mean difference in rotations (°) between model-based RSA and marker method RSA

†SD of the mean difference, random variation

‡limits of agreement (LoA) 95%, expected clinical precision

§minimum observed value

¶maximum observed value

Rx, Ry and Rz: mean difference in rotation errors around the x-, y- and z-axis, respectively

the controlled random search algorithm with local mutations (NLOPT\_GN\_CR2\_LM) was used.<sup>23</sup> Subsequently the registration was refined using the Sbpplx (NLOPT\_LN\_SBPLX) algorithm.<sup>24</sup>

**Statistical analysis.** Validation of MBM and DRR was done by comparing migration results, in all six degrees of freedom, for MBM and DRR individually with respect to MM as the benchmark reference. MBRSA was used to perform pairwise analyses of the same stereoradiographs analyzed by the different methods, thus describing the difference/error of MBM and DRR with respect to MM. For DRR pairwise migration was performed by entering the position of the bones achieved in the customized DRR analysis software, into MBRSA, so migration results were achieved equally for both methods. This was possible due to equal calibrations and aligned bone model coordinate systems.

Data is described as translation (mm) and rotation error (°) in six degrees of freedom for MBM and DRR. Data was summarized as means, limits of agreement (LoA) (LoA = mean  $\pm$  1.96  $\times$  standard deviation) and minimum and maximum values for all six degrees of freedom separately.<sup>25</sup> Systematic error was assessed as the mean of migration errors and precision, assessed as random error and assessed by 95% limits of agreement (LoA). Total translation and rotation error was defined as the difference in the norm of translations and rotations,

respectively. The norm was calculated using the 3D Pythagorean theorem ( $T^2 = X^2 + Y^2 + Z^2$ ), which is unproblematic to use for translations and allowed for small rotations.<sup>3,26</sup> To test for systematic error one sample *t*-tests of the means in all six degrees of freedom were performed to test if the means differed statistically significantly from 0. Pitman's test for equal variance was used to compare the precision of MBM and DRR. The test was rejected when a negative correlation was achieved. Bootstrap analyses were performed to justify the use of the *t*-test and Pitman's test for non-normally distributed data. Statistical significance was assumed at 5% and Stata 14.1 (StataCorp, College Station, Texas) was used for the statistical calculation.

## Results

A total of 288 dynamic RSA images were analyzed by MBM, DRR and MM and the migration error between methods calculated by pairwise migration (Tables I to IV). For the MM analysis, the mean rigid body error was 0.063 mm (95% confidence interval (CI) 0.059; 0.067 mm; minimum (min) = 0.014 mm, maximum (max) = 0.20 mm) and the mean condition number was 33.7 (95% CI 32.6; 34.7; min = 15.0, max = 51.5). Systematic bias for DRR and MBM with respect to MM in translations ( $\Delta < 0.18$  mm) and rotations ( $\Delta < 0.009^\circ$ ) were approximately 0. For fitting of the femur, the systematic bias of both methods

**Table III.** Digitally reconstructed radiograph (DRR); mean difference in translation errors, n = 288

	Femur				Pelvis			
	Tx	Ty	Tz	Total	Tx	Ty	Tz	Total
Mean difference <sup>a</sup>	0.006	0.018**	0.004	0.157	-0.001	0.001	0.000	0.050
SD difference <sup>†</sup>	0.057	0.078	0.162	0.107	0.022	0.022	0.056	0.040
± LoA <sup>‡</sup>	0.112	0.154	0.318	0.210	0.043	0.042	0.110	0.078
Minimum <sup>§</sup>	-0.207	-0.273	-0.457	0.009	-0.105	-0.0701	-0.215	0.003
Maximum <sup>¶</sup>	0.344	0.424	0.518	0.541	0.113	0.0776	0.218	0.226

<sup>a</sup>mean difference in translations (mm) between DRR and marker method radiostereometric analysis

<sup>†</sup>SD of the mean difference, random variation

<sup>‡</sup>limits of agreement (LoA) 95%, expected clinical precision

<sup>§</sup>minimum observed value

<sup>¶</sup>maximum observed value

\*\*statistically significantly different from 0, paired *t*-test

Tx, Ty and Tz: mean difference in translation errors along the x-, y- and z-axis, respectively

**Table IV.** Digitally reconstructed radiograph (DRR); mean difference in rotation errors, n = 288

	Femur				Pelvis			
	Rx	Ry	Rz	Total	Rx	Ry	Rz	Total
Mean difference <sup>a</sup>	0.005	0.004	0.003	0.221	-0.002	-0.000	0.002	0.101
SD difference <sup>†</sup>	0.153	0.187	0.108	0.146	0.083	0.088	0.052	0.084
± LoA <sup>‡</sup>	0.299	0.367	0.211	0.286	0.163	0.172	0.102	0.165
Minimum <sup>§</sup>	-0.488	-0.610	-0.382	0.015	-0.426	-0.319	-0.172	0.008
Maximum <sup>¶</sup>	0.634	0.556	0.395	0.834	0.449	0.279	0.194	0.556

<sup>a</sup>mean difference in rotations (mm) between DRR and marker method radiostereometric analysis

<sup>†</sup>SD of the mean difference, random variation

<sup>‡</sup>limits of agreement (LoA) 95%, expected clinical precision

<sup>§</sup>minimum observed value

<sup>¶</sup>maximum observed value

Rx, Ry and Rz: mean difference in rotation errors around the x-, y- and z-axis, respectively

was 0 in all degrees of freedom ( $p < 0.05$ ) but the Y-translation where it was approximately 0 for MBM (mean difference (diff) = 0.014 mm) and DRR (mean diff = 0.018 mm). For fitting of the pelvis systematic bias was 0 in all degrees of freedom (both rotation and translation) ( $p < 0.05$ ). Pitman's test was rejected for all degrees of freedom revealing lower random variation in all degrees of freedom for DRR compared with MBM ( $p < 0.001$ ).

**Precision of MBRSA.** LoA for the translation error of the femur ranged between 0.15 mm and 0.44 mm (min and max errors: -0.83; 0.67 mm), for the pelvis between 0.21 mm and 0.91 mm (min and max errors: -1.5; 1.9 mm) (Table I). LoA for femur rotation errors ranged between 0.37° and 0.71° (min and max error: -1.6°; 1.3°), and for the pelvis between 0.48° and 0.58° (min and max error: -1.2°; 1.4°) (Table II). The largest rotation errors were observed for the y-rotation of femur. For both bones the largest individual translation errors observed were along the z-axis.

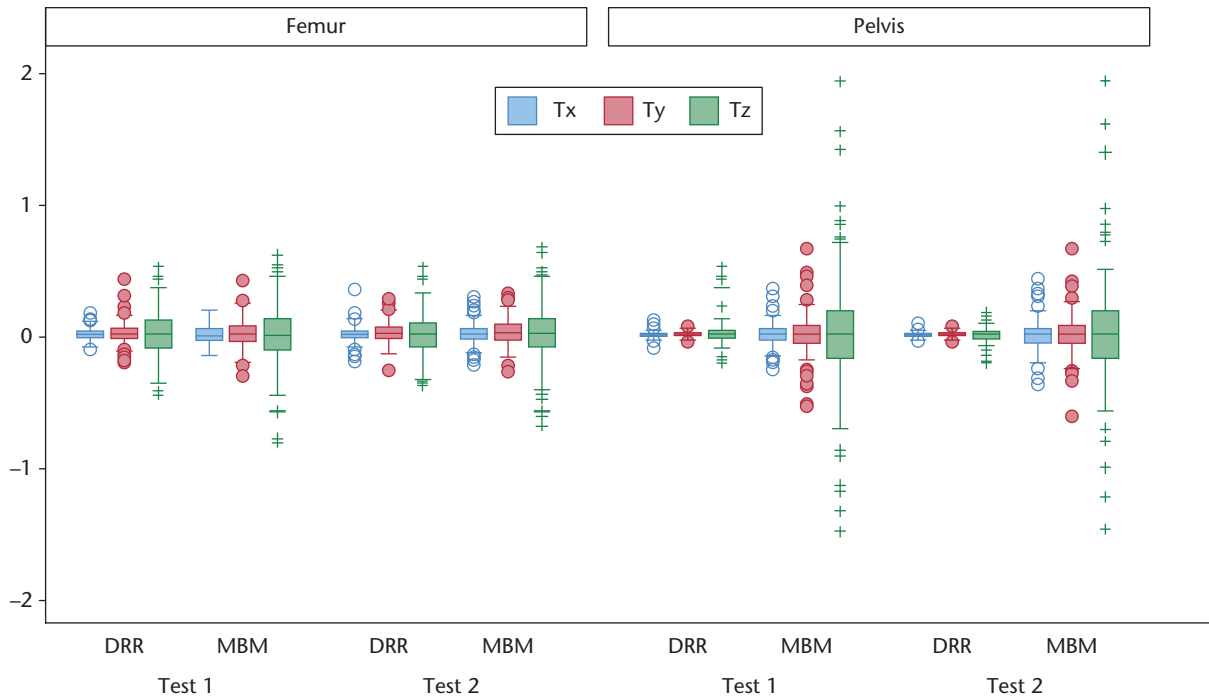
**Precision of DRRs.** LoA for the translation error of the femur ranged between 0.057 mm and 0.162 mm (min and max errors: -0.457; 0.518 mm), for the pelvis between 0.042 mm and 0.110 mm (min and max errors: -0.215; 0.218 mm) (Table III). LoA for femur rotation errors ranged between 0.37° and 0.71° (min and max error: -0.610°; 0.634°), and for the pelvis between

0.102° and 0.449° (min and max error: -0.426°; 0.449°) (Table IV). The largest rotation errors were observed for the x-rotation of femur. Like MBM, the largest individual translation errors observed for both bones were along the z-axis.

Bootstrapping was performed with 1000 samples from the migration data in each degree of freedom. The confidence intervals and p-values achieved by bootstrapping were compared with the results obtained by the paired *t*-test on the entire non-normally distributed dataset. No indication of non-normal distribution was found and therefore the results of the one-sample *t*-tests were accepted and found valid.

Figures 4 and 5 show boxplots over the migration data of DRR and MBM and shows that the quartile ranges of DRR are narrower in all degrees of freedom. Furthermore, it is observed that fewer outliers occur when analysing stereoradiographs by DRR.

Dose calculations were performed on real-time dynamic RSA recordings. The effective dose per exposure was 0.054 mSv. With a mean exposure time of 9 seconds and a framerate of 5 frames/sec the effective dose per recording is 2.43 mSv. Both the pre- and post-operative CT-scans contributed with an effective dose of 10 mSv. The total effective dose per specimen was 24.86 mSv.



Graphs by group(bone)

Fig. 4

Box plots of translation errors of the model-based method (MBM) and a digitally-reconstructed radiograph (DRR) with respect to benchmark marker based (MM) radiostereometric analysis (in mm) for Tx, Ty and Tz for the femur and the pelvis individually.

## Discussion

We performed a validation study of bone MBRSA applied to the native (non-prosthetic) hip joint, and assessed precision of MBM and DRR with respect to MM analysis as the benchmark. Bias between methods approximated 0. LoA for MBM were below 0.44 mm for translations of the femur, below 0.91 mm for translations of the pelvis and below  $0.7^\circ$  in rotations for both the femur and pelvis. Superior precision was achieved by DRR with LoA for translations below 0.32 mm and 0.11 mm and for rotations below  $0.36^\circ$  and  $0.17^\circ$  for the femur and pelvis, respectively.

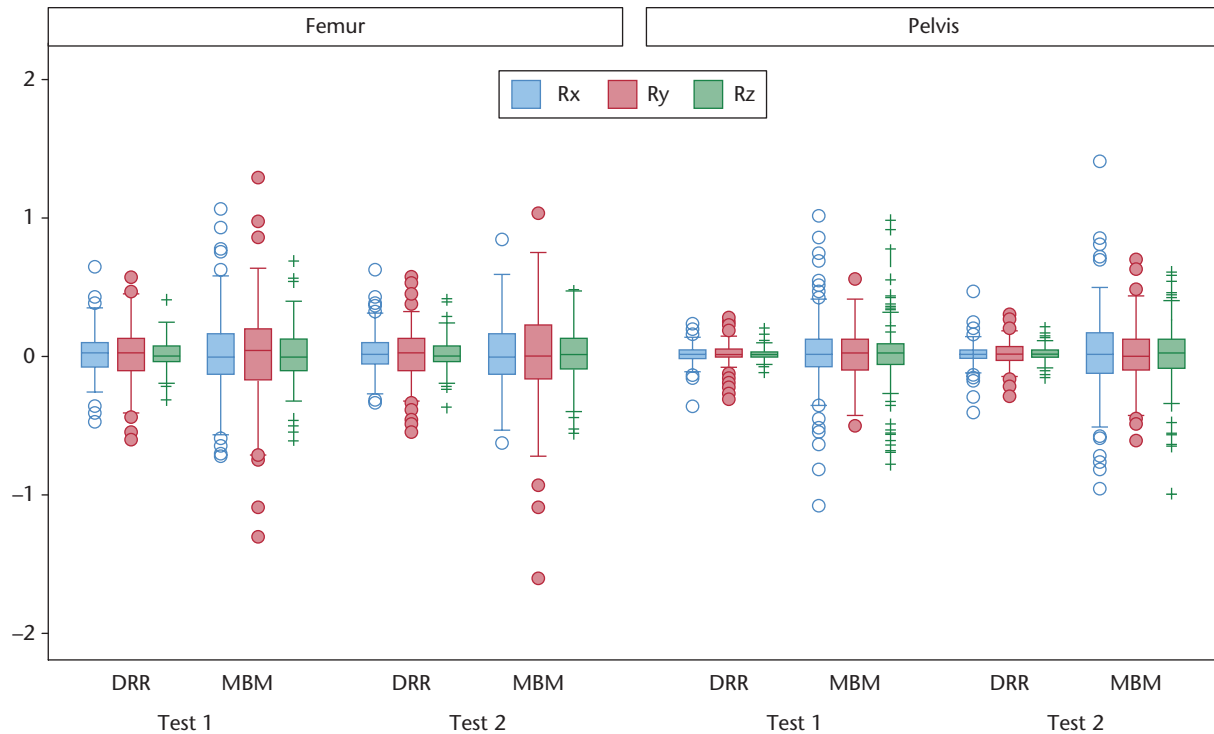
For the marker analyses the mean ME of 0.06 mm and the mean condition number of 34 was substantially below the recommended values and accordingly the quality of the MM analysis should be excellent.<sup>17,18</sup>

MM is the benchmark method for measuring *in vivo* micro movement and displacement of orthopaedic implants. Lorenzen et al<sup>27</sup> performed a phantom study of the hip, determining the precision (determined as SD) of MM on resurfacing hip implants to range between 0.02 mm to 0.07 mm for translations and  $0.05^\circ$  to  $0.11^\circ$  for rotations, which is extremely precise. Given the values of condition number in our study we assume that precision and accuracy of our analyses are comparable with the findings of Lorenzen et al.<sup>27</sup> Stilling et al<sup>28</sup> reported an overall precision of 0.19 mm of MBM applied for determining the position of hip implants. As our study

investigated the same anatomical region as Stilling et al,<sup>28</sup> it is expected that the same high precision of MM would be achieved.

A significant limitation of non-invasive bone MBMs of RSA of the hip and pelvis is the radiation dose received by patients during RSA-examinations and, more importantly, during CT scans used for bone model construction. Therefore, the dose the patient receives needs to be justified by the information that could possibly be gained from the examination. During our study a substantial dose reduction of the CT scans to 5.2 mSv for the preoperative scan was achieved along with further reduction for the postoperative scan. Dose reductions for the RSA recording can also be made. Reduction in the radiation dose will then justify the MBRSA methods in FAI patients, particularly when taking into account the severity and prevalence of FAI.<sup>29</sup>

Kapron et al<sup>30</sup> have performed a similar study validating a volume-based method using DRRs for tracking of the hip on two human donor specimens. The achieved precision (measured in SD) of translations for an anterior impingement test ranged between 0.38 mm and 0.59 mm and for angular measurements between  $0.44^\circ$  and  $0.74^\circ$ . Though not directly comparable, better results were achieved by the DRR method in this study. Kapron et al<sup>30</sup> also used MM as a reference but validated the method using an acrylic plate with incorporated markers. We used a MM that has been validated in clinically



Graphs by group(bone)

Fig. 5

Box plot of rotations errors of rotation errors for the model-based method (MBM) with respect to benchmark marker based (MM) radiostereometric analysis (°) for Rx, Ry and Rz for the femur and the pelvis individually.

relevant positions and therefore the precision results of our study should be of higher quality. Martin et al<sup>19</sup> have validated another DRR method for model-based tracking of the hip which also generally shows inferior precision results compared with the DRR method presented in this paper. Existing studies have validated RSA bone model methods for dynamic 3D tracking of the knee.<sup>10,31</sup> The MBM method presented in this study has previously been used to perform kinematic studies on donor hips and knees.<sup>6,8</sup>

Based on the data obtained in this study we can conclude that MBM and DRR can be applied for evaluation of hip joint kinematics with research relevant precision. DRR showed superior precision and will hence be a more suitable and even automated method for measuring end-range bone translations and bone-bone distances.

MBM and DRR are both non-invasive methods which make them suitable for diagnostic and preoperative, as well as postoperative, evaluations, in contrast to MM, which is only applicable postoperatively. However, compared with DRR, RSA analysis of bone models with MBRSA (RSACore) is more time consuming as it requires user interaction, which limits its applicability to small research studies with a limited number of images to analyze. In contrast, DRR could be useful in the clinic for analysis of

larger recordings as the method is automated and not user dependent.

In conclusion, DRR applied to the hip joint has shown highly sufficient precision to reveal valuable and clinically relevant information of hip joint kinematics including the native hip joint and diseased hip joints such as FAI and hip dysplasia.

Model-based tracking methods are also applicable to other joints that need evaluating. Notably the kinematic effects of surgery, analyzing joint pathomechanics and studying the consequences of trauma. However, individual validation studies are necessary before applying the method to a new joint, in order to know the precision, feasibility and limitations of the method in the specific anatomical region.

## References

1. Bojan AJ, Bragdon C, Jönsson A, Ekholm C, Kärrholm J. Three-dimensional bone-implant movements in trochanteric hip fractures: precision and accuracy of radiostereometric analysis in a phantom model. *J Orthop Res* 2015;33:705-711.
2. Kärrholm J. Roentgen stereophotogrammetry. Review of orthopedic applications. *Acta Orthop Scand* 1989;60:491-503.
3. Selvik G. Roentgen stereophotogrammetry. A method for the study of the kinematics of the skeletal system. *Acta Orthop Scand Suppl* 1989;232:1-51.
4. Kaptein BL, Valstar ER, Stoel BC, Rozing PM, Reiber JHC. A new model-based RSA method validated using CAD models and models from reversed engineering. *J Biomech* 2003;36:873-882.



5. **Valstar ER, de Jong FW, Vrooman HA, Rozing PM, Reiber JHC.** Model-based Roentgen stereophotogrammetry of orthopaedic implants. *J Biomech* 2001;34:715-722.
6. **Hansen L, Raedt S De, Jørgensen PB, Mygind-klavsen B, Kaptein B.** Dynamic radiostereometric analysis for evaluation of hip joint pathomechanics. *J Exp Orthop* 2017;4:20.
7. **Seehaus F, Olender GD, Kaptein BL, Ostermeier S, Hurschler C.** Markerless Roentgen Stereophotogrammetric Analysis for in vivo implant migration measurement using three dimensional surface models to represent bone. *J Biomech* 2012;45:1540-1545.
8. **Stentz-Olesen K, Nielsen ET, de Raedt S, et al.** Reconstructing the anterolateral ligament does not decrease rotational knee laxity in ACL-reconstructed knees. *Knee Surg Sports Traumatol Arthrosc* 2017;25:1125-1131.
9. **de Bruin PW, Kaptein BL, Stoel BC, et al.** Image-based RSA: roentgen stereophotogrammetric analysis based on 2D-3D image registration. *J Biomech* 2008;41:155-164.
10. **Stentz-Olesen K, Nielsen ET, De Raedt S, et al.** Validation of static and dynamic radiostereometric analysis of the knee joint using bone models from CT data. *Bone Joint Res* 2017;6:376-384.
11. **de Raedt S, Mechlenburg I, Stilling M, et al.** Automated measurement of diagnostic angles for hip dysplasia [abstract]. *SPIE Medical Imaging, International Society for Optics and Photonics*, 2013.
12. **Krčah M, Székely G, Blanc R.** Fully automatic and fast segmentation of the femur bone from 3D-CT images with no shape prior [abstract]. *Biomedical Imaging: From Nano to Macro, IEEE International Symposium*, 2011.
13. **Boykov Y, Funka-Lea G.** Graph cuts and efficient N-D image segmentation. *Int J Comput Vis* 2006;70:109-131.
14. **Wu G, Siegler S, Allard P, et al.** Standardization and Terminology Committee of the International Society of Biomechanics; International Society of Biomechanics. ISB recommendation on definitions of joint coordinate system of various joints for the reporting of human joint motion—part I: ankle, hip, and spine. *J Biomech* 2002;35:543-548.
15. **Baker R.** ISB recommendation on definition of joint coordinate systems for the reporting of human joint motion—part I: ankle, hip and spine. *J Biomech* 2003;36:300-302.
16. **Griffin DR, Dickenson EJ, O'Donnell J, et al.** The Warwick Agreement on femoroacetabular impingement syndrome (FAI syndrome): an international consensus statement. *Br J Sports Med* 2016;50:1169-1176.
17. **Valstar ER, Gill R, Ryd L, et al.** Guidelines for standardization of radiostereometry (RSA) of implants. *Acta Orthop* 2005;76:563-572.
18. **Söderkvist I, Wedin PA.** Determining the movements of the skeleton using well-configured markers. *J Biomech* 1993;26:1473-1477.
19. **Martin DE, Greco NJ, Klatt BA, et al.** Model-based tracking of the hip: implications for novel analyses of hip pathology. *J Arthroplasty* 2011;26:88-97.
20. **Kaptein BL, Valstar ER, Stoel BC, Rozing PM, Reiber JHC.** Evaluation of three pose estimation algorithms for model-based roentgen stereophotogrammetric analysis. *Proc Inst Mech Eng H* 2004;218:231-238.
21. **van der Bom IMJ, Klein S, Staring M, et al.** Evaluation of optimization methods for intensity-based 2D-3D registration in x-ray guided interventions. *Proc SPIE* 2011;7962:796223, 796223-15.
22. **Klein S, Staring M, Murphy K, Viergever MA, Pluim JPW.** elastix: a toolbox for intensity-based medical image registration. *IEEE Trans Med Imaging* 2010;29:196-205.
23. **Kaelo P, Ali MM.** Some Variants of the Controlled Random Search Algorithm for Global Optimization. *J Optim Theory Appl* 2006;130:253-264.
24. **Rowan T.** *Functional Stability Analysis of Numerical Algorithms*. Austin: University of Texas, 1990.
25. **Altman DG.** *Practical Statistics for Medical Research*. London: Chapman & Hall, 1991:1-6.
26. **Kaptein BL, Valstar ER, Stoel BC, Reiber HC, Nelissen RG.** Clinical Validation of Model-based RSA for a Total Knee Prosthesis. *Clin Orthop Relat Res* 2017;464:205-209.
27. **Lorenzen ND, Stilling M, Jakobsen SS, et al.** Marker-based or model-based RSA for evaluation of hip resurfacing arthroplasty? A clinical validation and 5-year follow-up. *Arch Orthop Trauma Surg* 2013;133:1613-1621.
28. **Stilling M, Kold S, de Raedt S, et al.** Superior accuracy of model-based radiostereometric analysis for measurement of polyethylene wear: A phantom study. *Bone Joint Res* 2012;1:180-191.
29. **Directorate-General Environment, Nuclear Safety, and Civil Protection, European Commission.** Radiation protection 99: Guidance on medical exposures in medical and biomedical research, 1998. [https://ec.europa.eu/energy/sites/ener/files/documents/099\\_en.pdf](https://ec.europa.eu/energy/sites/ener/files/documents/099_en.pdf) (date last accessed 09 May 2018).
30. **Kapron AL, Aoki SK, Peters CL, et al.** Accuracy and feasibility of dual fluoroscopy and model-based tracking to quantify in vivo hip kinematics during clinical exams. *J Appl Biomech* 2014;30:461-470.
31. **Anderst W, Zauel R, Bishop J, Demps E, Tashman S.** Validation of Three-Dimensional Model-Based Tibio-Femoral Tracking During Running. *Med Eng Phys* 2009;31:10-16.

#### Funding Statement

- This work was supported by The Novo Nordisk Foundation grant number 17576, The Danish Rheumatism Association grant number R141-A3998, Orthopaedic Research Foundation, Aarhus and The Danish Orthopaedic Society Foundation.

#### Author Contributions

- L. Hansen: Research design, Data acquisition, Analysis and interpretation, Writing of the first manuscript draft.
- S. De Raedt: Research design, Data analysis and interpretation, Critical revisions of the manuscript.
- P. B. Jørgensen: Research design, Data acquisition, Radiographic analyses.
- B. Mygind-Klavsen: Performed surgery, Data acquisition, Critical review.
- B. Kaptein: Data analysis and interpretation, Critical revisions of the manuscript.
- M. Stilling: Research design, Data acquisition and interpretation, Critical revisions of the manuscript.

#### Conflict of Interest Statement

- None declared

© 2018 Author(s) et al. This is an open-access article distributed under the terms of the Creative Commons Attribution licence (CC-BY-NC), which permits unrestricted use, distribution, and reproduction in any medium, but not for commercial gain, provided the original author and source are credited.